Semiconductor Conjugated Polymer−Quantum Dot Nanocomposites at the Air/Water Interface and Their Photovoltaic Performance

Matthew D. Goodman, Jun Xu, Jun Wang, and Zhiqun Lin*

Department of Materials Science and Engineering, Iowa State University, Ames, Iowa 50011

Received December 2, 2008. Revised Manuscript Received December 18, 2008

Organic−inorganic nanocomposites consisting of electroactive conjugated polymer, poly(3-hexylthiophene) (P3HT), intimately tethered on the surface of semiconductor CdSe quantum dot (i.e., P3HT−CdSe nanocomposites) at the air/water interface formed via Langmuir isotherms were explored for the first time. The P3HT−CdSe nanocomposites displayed a high pressure plateau (∼10.5 mN/m) in the Langmuir isotherm, illustrating their complex packing at the air/water interface. The packing of the Langmuir−Blodgett (LB) depositions of nanocomposites was revealed by AFM measurements. Furthermore, photovoltaic devices fabricated from the LB depositions of the P3HT−CdSe nanocomposites exhibited a relatively high short circuit current, I_{SC}, while maintaining a thin film profile. These studies provide insights into the fundamental behaviors of semiconductor organic−inorganic nanocomposites confined at the air/water interface as well as in the active layer of an organic-based photovoltaic device.

Introduction

Composites of semiconductor quantum dot (QD)[1−3] and electroactive conjugated polymer (CP)[4−6] have been the focus of intense study due to the unique and promising photophysical properties for use in optoelectronic devices.[7−9] They are often prepared by physically mixing CP and QD or by constructing a CP/QD bilayer or CP/QD multilayer, in which only a small fraction of excitons, that is, the bound electron−hole pairs, are able to diffuse to the interface at which they are dissociated.[10] By contrast, only a few elegant studies have been done on CP-QD nanocomposites, in which the CP is intimately tethered to the QD. Such direct attachment of the CP to the QD via ligand exchange with insulate surfactants[11−13] or direct growth from/onto the QDs' surface[14,15] affords a more controlled interface on a molecular scale and morphology, thereby allowing for efficient charge or energy transfer between these two constituents. For example, oligo(phenylene vinylene) was directly grown from [(4-bromophenyl)methyl]dioctylphosphine oxide (DOPO-Br)-functionalized CdSe QD for efficient energy transfer; suppressed blinking from the CdSe QD was observed.[14,16] Recently, the P3HT−CdSe nanocomposites were synthesized by directly grafting a comparatively long, vinyl-terminated regioregular poly(3-hexylthiophene) (P3HT) onto the (DOPO-Br)-functionalized CdSe QD surface via a mild palladium-catalyzed Heck coupling, dispensing with the need for ligand exchange chemistry.[15] The charge transfer from P3HT to CdSe QDs was observed, as confirmed by the emission spectra and fluorescence lifetime measurements.[15]

Several fabrication techniques are widely used to make thin organized organic/inorganic composite films including spin coating, Langmuir−Blodgett (LB) depositions, and layer-by-layer (LbL) assembly.[17,18] To the best of our knowledge, the only previous work of a photovoltaic device using semiconductor conjugated polymer-quantum dot (i.e., P7T-CdSe) nanocomposites as the active layer was done by Advincula.[13] The P7T-CdSe nanocomposites were produced via substituting the pyridine-capped CdSe QDs for 2,3-di(5,5″-dihexyl-[2,2′;3′,2″]terthiophene-5′-yl)thiophene-ylphosphonic acid (P7T); that is, a ligand exchange method. The thin film photovoltaic device was fabricated by spin-coating P7T-CdSe nanocomposites on the indium tin oxide (ITO) glass.[13] Notably, the power conversion efficiency, PCE = 0.2%, was obtained at the power of incident light, P_{inc} = 0.1 mW/cm^2, instead of the commonly used P_{inc} = 100 mW/cm^2, presumably because of the limited absorption capacity of thin photovoltaic device. Herein, we report the first study of the behavior of P3HT−CdSe nanocomposites, which were

* To whom correspondence should be addressed. E-mail: zqlin@iastate.edu.

(1) Xu, J.; Xia, J.; Lin, Z. Q. *Angew. Chem., Int. Ed.* **2007**, *46*, 1860.
(2) Xu, J.; Xia, J. F.; Wang, J.; Shinar, J.; Lin, Z. Q. *Appl. Phys. Lett.* **2006**, *89*, 133110.
(3) Wang, J.; Xu, J.; Goodman, M. D.; Chen, Y.; Cai, M.; Shinar, J.; Lin, Z. Q. *J. Mater. Chem.* **2008**, *18*, 3270.
(4) Schwartz, B. J. *Annu. Rev. Phys. Chem.* **2003**, *54*, 141.
(5) Xu, J.; Xia, J.; Hong, S. W.; Lin, Z. Q.; Qiu, F.; Yang, Y. L. *Phys. Rev. Lett.* **2006**, *96*, 066104.
(6) Lin, Y.-H.; Jiang, C. Y.; Xu, J.; Lin, Z. Q.; Tsukruk, V. V. *Adv. Mater.* **2007**, *19*, 3827.
(7) Colvin, V. L.; Schlamp, M. C.; Alivisatos, A. P. *Nature* **1994**, *370*, 354.
(8) Coe, S.; Woo, W. K.; Bawendi, M.; Bulovis, V. *Nature* **2002**, *420*, 800.
(9) Huynh, W. U.; Dittmer, J. J.; Alivisatos, A. P. *Science* **2002**, *295*, 2425.
(10) Lin, Z. Q. *Chem. Eur. J.* **2008**, *14*, 6294.
(11) Milliron, D. J.; Alivisatos, A. P.; Pitois, C.; Edder, C.; Frechet, J. M. J. *Adv. Mater.* **2003**, *15*, 58.
(12) Milliron, D. J.; Gur, I.; Alivisatos, A. P. *MRS Bull.* **2005**, *30*, 41.
(13) Advincula, R. C. *Dalton Trans.* **2006**, 2778.
(14) Skaff, H.; Sill, K.; Emrick, T. *J. Am. Chem. Soc.* **2004**, *126*, 11322.
(15) Xu, J.; Wang, J.; Mitchell, M.; Mukherjee, P.; Jeffries-EL, M.; Petrich, J. W.; Lin, Z. Q. *J. Am. Chem. Soc.* **2007**, *129*, 12828.
(16) Hammer, N. I.; Early, K. T.; Sill, K.; Odoi, M. Y.; Emrick, T.; Barnes, M. D. *J. Phys. Chem. B* **2006**, *110*, 14167.
(17) Zimnitsky, D.; Jiang, C.; Xu, J.; Lin, Z. Q.; Tsukruk, V. V. *Langmuir* **2007**, *23*, 4509.
(18) Zimnitsky, D.; Jiang, C.; Xu, J.; Lin, Z. Q.; Zhang, L.; Tsukruk, V. V. *Langmuir* **2007**, *23*, 10176.

10.1021/cm803248j CCC: $40.75
Published on Web 01/26/2009

synthesized via directly tethering P3HT onto CdSe surface, at the air/water interface. Subsequently, the P3HT−CdSe nanocomposite monolayer depositions prepared by Langmuir−Blodgett (LB) method were incorporated into a thin film photovoltaic device. The performance of the resulting photovoltaic device was investigated. These studies provide insight into the fundamental behaviors of semiconductor organic−inorganic nanocomposites confined at the air/water interface as well as in the active layer of an organic-based photovoltaic device.

Experimental Section

Langmuir Isotherms and LB Depositions of the P3HT−CdSe Nanocomposites. The P3HT−CdSe nanocomposite was synthesized via a mild Heck coupling, as previously reported by our group.[15] Briefly, 3.5 nm CdSe QD functionalized with [(4-bromophenyl)methyl]dioctylphosphine oxide (DOPO-Br) was coupled with vinyl-terminated poly(3-hexylthiophene) (P3HT) (MW = 2404 g/mol, PDI = 1.12). The CdSe QD was grafted with 22 P3HT chains as determined by thermogravimetry analysis (TGA).[15] The resulting nanocomposites were precipitated twice with a minimal amount of methanol, centrifuged, and dissolved in chlorobenzene (concentration, c = 0.2 mg/mL). Langmuir isotherms (i.e., pressure−area, π−A isotherms) and LB depositions were conducted on an R&K-1 trough (Riegel & Kirstein, GmbH) with 5−10 uniform drops, 15−30 μL in total, evenly distributed on the water subphase (NanoPure, 18.2 MΩ·cm). After complete evaporation of chlorobenzene, approximately 45 min, Langmuir isotherms were recorded while compressing at a rate of 150 μm/s. The LB depositions were conducted by keeping the surface pressure constant while lifting the clean ITO substrate from the water subphase at a rate of 35 μm/s.

AFM Images of LB Depositions. AFM images were taken in tapping mode on a Dimension 3000 (Veeco) in the "light" tapping regime as to not damage the monolayer.[19] BS-tap300 tips (Budget Sensors) with spring constants ranging from 20 to 75 N m^{-1} were used as scanning probes. Scan rates were kept between 0.8 and 1.1 Hz for all imaging.

Fabrication of Photovoltaic Devices. LB multilayers of the P3HT−CdSe nanocomposites were utilized in the fabrication of the photovoltaic device. Clean ITO glasses were withdrawn from the water subphase, allowed to dry, dipped back into the subphase at the same speed, and withdrawn, and this repeated once more for a total of five withdrawing-dipping cycles. Highly polished [111] Si wafers were cut into rectangular pieces with Al strips evaporated onto the wafers for use as the back electrode (Al-coated Si). The Al coated face was pressed on the P3HT−CdSe multilayers, annealed for 1 h at 120 °C under Ar, and sealed. The current−voltage (I−V) curves were recorded using a Keithley 2400 multisource meter illuminated with a solar simulator (air mass 1.5 global, AM 1.5G illumination, the power of incident light, P_{inc} = 100 mW/cm^2).

Results and Discussion

Langmuir isotherms (i.e., pressure−area, π−A isotherms) and LB depositions were conducted on an R&K-1 trough. The molecular weight of P3HT was 2404, corresponding to approximately 14 repeat units for a chain length of roughly 10.4 nm, given that the length of a single thiophene repeat unit is 0.74 nm.[15,20] This is relatively longer than the effective conjugation length, which is approximately 9−10 repeat units.[21,22] The regioregularity was previously confirmed to be greater than 94%, as determined by ^{1}H NMR.[15] The P3HT chains can be considered as rigid rods, at least initially, that is, in dilute solutions or before compression in LB trough. In this regard, the P3HT chains cannot easily collapse on the CdSe surface to form a dense shell layer, as is the case in flexible homopolymers, with the P3HT−CdSe nanocomposites being viewed as a "crouched hedgehog". Thus, the resulting diameter of the spherical nanocomposites is approximately 24.3 nm (i.e., two 14 × 0.74 = 10.4 nm long P3HT chains and a 3.5 nm CdSe QD).

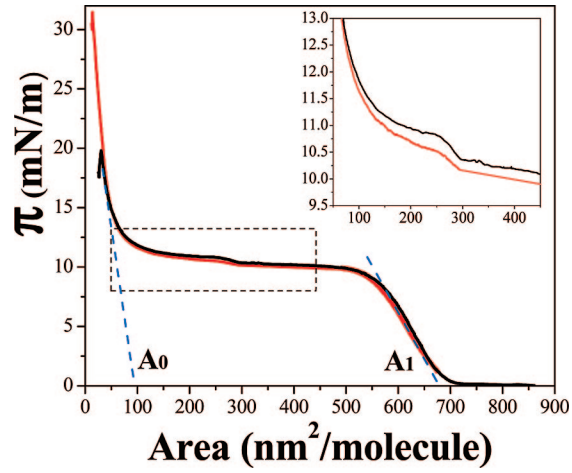

Figure 1. Pressure−area isotherm of the Langmuir monolayer of P3HT−CdSe nanocomposites. Single isotherm (black curve) and reversibility study (red curve). The extrapolation of the intial rise in pressure from 0 to 10 mN/m yielded the initial area, A_1. The limiting surface area, A_0, was obtained from the extrapolation of the sharp rise in pressure from 13 mN/m to monolayer collapse. The inset shows the pressure increase during the compression from 450 to 50 nm^2/molecules; at the pressure of 10.5 mN/m, the P3HT chains twisted at the conjugation length, forming interchain π−π stacking (Figure 2b).

Figure 1 depicts a typical Langmuir isotherm (black curve) as well as a reversibility study, i.e., compressing to 10 mN/m corresponding to 400 nm^2/molecule in area, expanding, another compression/expansion cycle, and then continuing to monolayer collapse (red curve). It is clear that during initial packing (i.e., from 0 to 10 mN/m), the nanocomposites exhibited complete reversibility; comparing the black curve with the red curve, the slight hysteresis can be attributed to the water subphase evaporation. From the isotherm, the initial area, A_1, can be determined by extrapolating the initial rise in pressure, that is, from 0 to 10 mN/m, while the limiting surface area, A_0, was calculated from the extrapolation of the sharp rise in pressure when the nanocomposites are in the condensed monolayer state, that is, from 13 mN/m to monolayer collapse. The initial area A_1 was found to be 686 nm^2, corresponding to a diameter of 29.5 nm, agreeing with the above prediction of 24.3 nm.

The small discrepancy between the measured (29.5 nm) and the predicted (24.3 nm) diameters can be attributed to

(19) Zimnitsky, D.; Xu, J.; Lin, Z. Q.; Tsukruk, V. V. *Nanotechnology* **2008**, *19*, 215606.
(20) Terada, Y.; Choi, B. K.; Heike, S.; Fujimori, M.; Hashizume, T. *Nano Lett.* **2003**, *3* (4), 527–531.
(21) Holdcroft, S. *Macromolecules* **1991**, *24*, 4834.
(22) Perepichka, I. F.; Perepichka, D. F.; Meng, H.; Wudl, F. *Adv. Mater.* **2005**, *17*, 2281.

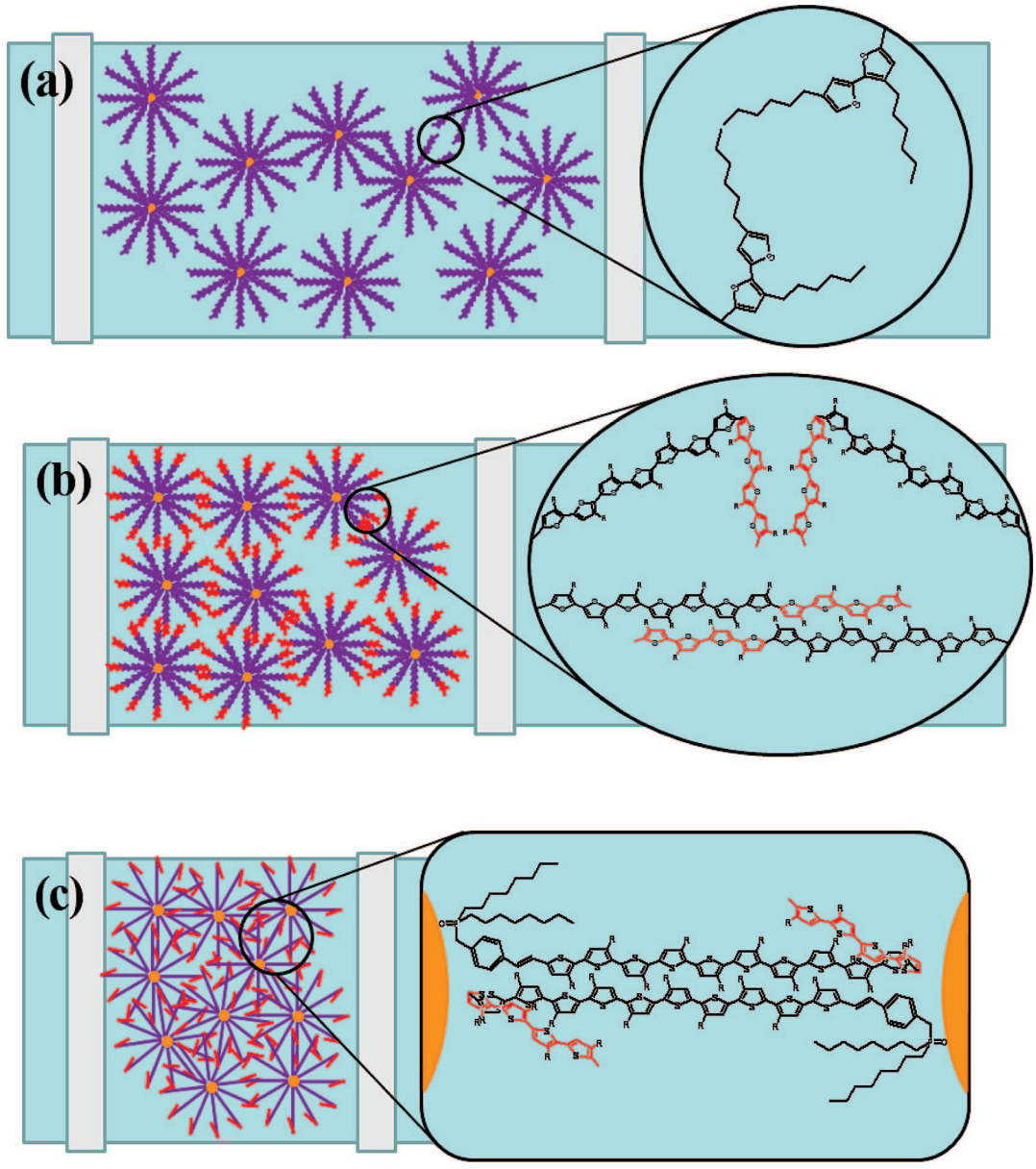

Figure 2. Schematic illustration of packing of the Langmuir monolayer of P3HT−CdSe nanocomposites at the air/water interface. The conjugation length of P3HT is approximately 10 thiophene units (black units) with the remaining denoted by the red units in (b) and (c). (a) The initial area, corresponding to the initial rise in pressure, in the Langmuir isotherm may be attributed to the interaction of the hexyl side chains in P3HT as well as the voids in the monolayer due to the spherical shape of the nanocomposites. (b) As area decreased during the compression, the P3HT chains bent and folded at the conjugation length. (c) Further decrease in area resulted in the interdigitation of P3HT chains from adjacent nanocomposites, causing a sharp rise in pressure and eventual monolayer collapse.

the following two factors. First, the P3HT chain was coupled to the DOPO-Br on the CdSe QD surface. The size of DOPO-Br was not included in the estimation of the QD size in the TEM measurements. Second, the P3HT−CdSe nanocomposites were in a spherical shape, so voids would inevitably be present in the nanocomposite monolayer due to the incomplete packing of rigid P3HT chains at low pressures (Figure 2a), resulting in an overestimation in the initial area, A_1. The hexyl side chains on P3HT from the neighboring nanocomposites may protrude beyond the thiophene unit length and interact with one another, leading to the rise in pressure (Figure 2a).

The slight increase in pressure, shown in the inset in Figure 1, around an area of 263 nm^2, corresponded to a nanocomposite diameter with the P3HT chains bent or folded at their conjugation length of 9−10 repeat units (i.e., $\pi(D/2)^2 = \pi[(3.5 + 0.74 \times 10 \times 2)/2]^2 = 262.9$ nm^2). As the monolayer was compressed, the P3HT chains from different nanocomposites can form $\pi-\pi$ stacking readily with the final 4−5 repeat units (red units), with the remaining 9−10 units (black units; the conjugation length) remaining rigid.[21,22] This is due to the already twisted backbone of the final repeat units (i.e., out-of-plane units), allowing the ease of further twisting (i.e., bending or folding) upon compression. Some chains may have the direct $\pi-\pi$ stacking (lower right close-up in Figure 2b); the others may bend slightly at the conjugation length to accomplish $\pi-\pi$ stacking due to the direct attachment and rigidity of the P3HT chains (upper right close-up in Figure 2b). Once the chains reached the conjugation length, continuing compression of the monolayer resulted in an increased pressure as the P3HT chains can no longer easily bend. This compression led to a jump in pressure and

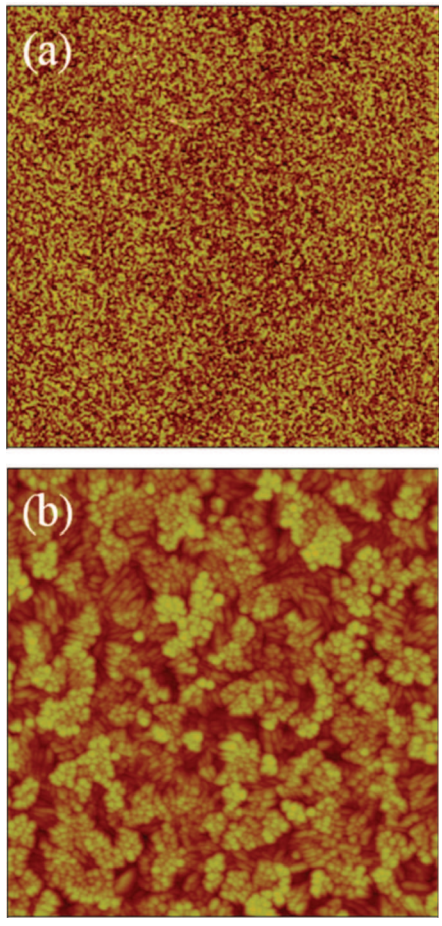

Figure 3. AFM height images of the Langmuir monolayer of P3HT−CdSe nanocomposites at the compression pressure of 10.5 mN/m. (a) Scan size = 20 μm and (b) scan size = 2 μm.

pushed the nanocomposites into the condensed monolayer state and eventual monolayer collapse.

Taken from the isotherms, the limiting surface area, A_0, was found to be 96 nm^2, corresponding to a nanocomposite diameter of 11 nm. Quite intriguingly, this diameter coincided well with the CdSe QD core (3.5 nm) plus two P3HT chains each 5 units long, which is half the conjugation length (3.5 + 2 × 5 × 0.74 = 10.9 nm; alternatively, the center to center distance between CdSe cores is 3.5/2 + 10 × 0.74 + 3.5/2 = 10.9 nm). This led us to propose that the P3HT chains did not bend or fold beyond the conjugation length of 9−10 repeat units but rather interdigitated with adjacent nanocomposites, forming interchain $\pi-\pi$ stacking to minimize the energy of the P3HT chains (Figure 2c). Since there were only 22 P3HT chains bound to the CdSe surface,[15] there was ample space for the polymer chains to penetrate and push against the CdSe core of adjacent nanocomposite. Once the chains reached the QD, the nanocomposites cannot compress anymore, causing a sharp rise in pressure and eventual monolayer collapse (Figure 2c).

AFM imaging was performed on the LB deposition samples taken from pressures of 5, 10.5, and 15 mN/m on ITO. Two representative AFM height images of a nanocomposite monolayer formed at 10.5 mN/m are shown in Figure 3. For the 20 μm scan, the root-mean-square (rms) roughness was found to be 3.821 nm (Figure 3a); the 2 μm scan had an rms roughness of 4.686 nm (Figure 3b). As a result of the length of the P3HT chains, only 14 repeat units, and being intimately connected to the QD, no long fiber-like morphologies were observed at any of the pressures. Instead, spherical nanocomposites can be seen at all pressures. The size of the nanocomposites measured laterally from the AFM images agreed with the area given by the Langmuir isotherm (Figure 3b). The thickness of the nanocomposites was determined by a scratch test on the 10.5 mN/m sample, yielding 11 nm. Clearly, the hydrophobic P3HT chains partially collapsed on the surface after the ITO substrate withdrawal. With the hydrophilic CdSe core and assumed uniform coverage of the P3HT chains, the chains that were attached below the core collapsed on the core surface in the water subphase due to their hydrophobicity. When the ITO substrate was removed from the trough, the CdSe core was situated on a layer of collapsed P3HT chains; the remaining chains were still rigid with the only bending or folding occurred at the conjugation length, that is, 3.5 nm CdSe core + 7.4 nm 10-unit P3HT = 10.9 nm thick, correlating well with the 11 nm thickness value measured experimentally. Figure 3b shows that upon compression and substrate withdrawal, most individual nanocomposites remained distinct in terms of the shape of the nanocomposites and the boundary between adjacent nanocomposites, with a few having an oblong profile. This profile may be a result of two or more nanocomposites partially interdigitating.

It is worth noting that although the P3HT−CdSe nanocomposites maximized the interface between the electron-donating P3HT and electron-accepting CdSe (i.e., $p-n$ junction) and provided a fast exciton dissociation, which are favorable for photovoltaic devices, no direct percolation between the CdSe QDs and the electrodes existed in spin-coated nanocomposite films. As a result, we observed a quite low photovoltaic performance of a spin-coated P3HT−CdSe film (PCE = 0.003%), similar to a pure P3HT film. To this end, LB depositions were utilized in the fabrication of a *thin* photovoltaic device to possibly achieve a direct pathway for CdSe QDs, as illustrated in Figure 4a. Although directly evaporating Al onto the LB film would provide a better contact between the Al electrode and the active layer, thus improving the device performance, the Al coated Si was used as the back electrode because the direct evaporation of Al always caused a device short. This can be explained due to the presence of nanoscopic voids in the monolayer as a consequence of the spherical nanocomposite packing described above (Figures 2 and 3), making the evaporated Al in direct contact with the ITO substrate.

The photovoltaic device performance of LB multilayers of nanocomposites under AM 1.5G illumination (the power of incident light, P_{inc} = 100 mW/cm^2) is shown in Figure 4b. The AFM scratch tests of the five-cycle multilayer deposition yielded an active layer thickness of approximately 30 nm, clearly indicating that the P3HT chains must collapse forming the $\pi-\pi$ stacking to accommodate five layers of the nanocomposites as depicted in Figure 4a. This is in contrast to a linear LB deposition, where the resulting five-layer structure would be approximately 50 nm (i.e., 5 layers × 11 nm for each layer). The $\pi-\pi$ stacking allowed for the

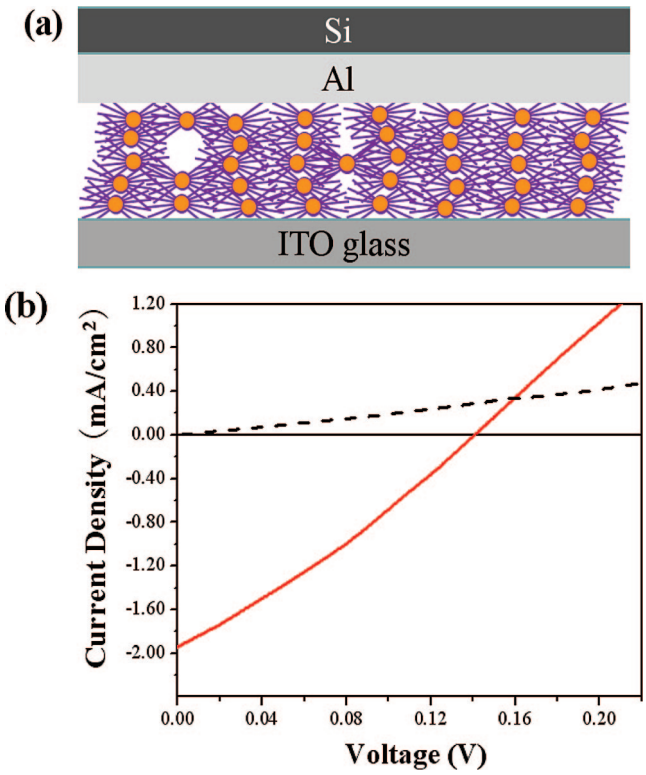

Figure 4. (a) Cross-sectional view of a multilayer (i.e., five monolayers) photovoltaic device. The ITO substrate was dipped into the LB trough repeatedly five times, depositing the P3HT−CdSe nanocomposites. The majority of P3HT chains folded at the conjugation length, with a few hydrophobic P3HT chains under the CdSe core collapsing to the CdSe surface while in the water subphase, yielding a 30 nm thick film. Al was evaporated onto a Si substrate and pressed on the 30 nm thick active layer. The resulting device was annealed at 120 °C for 1 h. (b) The current−voltage characteristic of the LB fabricated photovoltaic device (dashed line: in the dark; solid line: under illumination).

interaction between polymer chains of different nanocomposites, thereby providing a direct pathway for the holes to the electrode (Figure 4a). From the $I-V$ curve, the short circuit, $I_{SC} = 1.95$ mA/cm^2, and the open circuit voltage, $V_{OC} = 0.141$ V, can be obtained. Accordingly, the fill factor, defined as the ratio of maximum output power to input power, FF $= I_{max}V_{max}/(I_{SC}V_{OC})$ can be calculated to be 27.0%, where I_{max} and V_{max} are the current and voltage at maximum output power. Thus, PCE $= I_{SC}V_{OC}$FF$/P_{inc}$ was 0.08%.

The low performance can be rationalized as follows. First, the ultrathin photovoltaic device (i.e., a multilayer film of 30 nm thick) had relatively high I_{SC}, while the V_{OC} was low. This indicated that the contact between the active layer and the Al electrode was not perfect, despite the fact that the as-prepared photovoltaic device was annealed at 120 °C, which was well above the T_g of P3HT yet below its decomposition temperature.[23] It was originally anticipated that the thermal annealing would improve the device performance by allowing the P3HT chains to form the $\pi-\pi$ stacking between chains as well as facilitating the contact with the Al electrode;[24,25] thus, apparently, the temperature employed, 120 °C, cannot create a high-quality contact between Al and the active layer. Second, the 30-nm thick active layer may result in low light absorption and thus low PCE. Third, as noted above, a thin layer of collapsed P3HT was present between the ITO electrode and the CdSe core; however, with the grafting density of 22 P3HT chains, only a small portion of the core was blocked due to the P3HT with the remaining CdSe contacting the ITO. Thus, the hydrophilic *n*-type CdSe core was deposited on the hole-conducting ITO electrode while the electron-conducting Al electrode was pressed on the collapsed *p*-type P3HT, since the ITO glass was employed as the LB substrate (Figure 4a). For increased performance, the CdSe core should be in contact with the Al electrode for efficient electron collection while the P3HT chains are in contact with the ITO electrode for efficient hole collection. We note that in attempting LB deposition on the Al-coated Si with ITO pressed on the P3HT−CdSe multilayers, the device exhibited a dramatically decreased performance. This can be attributed to the insulating Al_2O_3 growth on Al that occurred after removal from the inert Ar glovebox environment. The final reason responsible for the low photovoltaic performance may be the lack of hole-conducting poly(3,4-ethylenedioxythiophene) (PEDOT) coating on the ITO electrode. A PEDOT-coated ITO substrate could not be utilized due to the solubility of the PEDOT in the water subphase, since the substrate was to be withdrawn from the LB trough. In the studies of using the Al-coated Si as the LB substrate, PEDOT was spin-coated on the ITO substrate; however, as noted earlier, the formed insulating Al_2O_3 layer on the Al surface decreased the overall performance of the resulting photovoltaic device.

In summary, semiconductor P3HT−CdSe nanocomposites at the air/water interface formed via Langmuir isotherms were explored for the first time. The size of the nanocomposites determined from the Langmuir isotherms agreed well with the prediction. The packing of the nanocomposites was complex with the P3HT chain folding and bending most easily at its conjugation length but did not fold nor collapse beyond that length. AFM measurements on the nanocomposite monolayer showed distinct nanocomposites on the substrate with most retaining the spherical shape. Photovoltaic devices fabricated from five LB deposition cycles of the P3HT−CdSe nanocomposites, approximately 30 nm thick, exhibited a relatively high short circuit current, I_{SC}, while maintaining an ultrathin film profile, yielding a PCE of 0.08%. On the basis of these results, we envision that improved photovoltaic performance may be achieved by introducing QDs into CP-QD nanocomposites via forming a better percolation for charge transport. This work is currently under investigation.

Acknowledgment. We gratefully acknowledge support from the National Science Foundation (NSF-CBET 0824361) and 3M.

CM803248J

(23) Kuila, B. K.; Malik, S.; Batabyal, S. K.; Nandi, A. K. *Macromolecules* **2007**, *40* (2), 278–287.

(24) Kim, Y.; Cook, S.; Tuladhar, S. M.; Choulis, S. A.; Nelson, J.; Durrant, J. R.; Bradley, D. D. C.; Giles, M.; Mcculloch, I.; Ha, C. S.; Ree, M. *Nat. Mater.* **2006**, *5*, 197.

(25) Yang, X.; Loos, J.; Veenstra, S. C.; Verhees, W. J. H.; Wienk, M. M.; Kroon, J. M.; Michels, M. A. J.; Janssen, R. A. J. *Nano Lett.* **2005**, *5*, 579.